2000

Blending of Immiscible Polymers in a Mixing Zone of a Twin Screw Extruder- Effects of Compatibilization

William MacKnight, *University of Massachusetts Amherst*
O. Franzheim
T. Rische
M. Stephan

Blending of Immiscible Polymers in a Mixing Zone of a Twin Screw Extruder—Effects of Compatibilization

O. FRANZHEIM,[1*] T. RISCHE,[1] M. STEPHAN,[1] *and* W. J. MACKNIGHT[2]

[1]*Institute of Polymer Research Dresden e. V.*
Hohe Str. 6
D-01069 Dresden, Germany

[2]*University of Massachusetts at Amherst*
Dept. Polymer Science and Engineering
Amherst, Massachusetts, 01003

[*]*Werner & Pfleiderer GmbH*
Theodorstr. 10
D-70469 Stuttgart, Germany

The dependence of the morphology development of physical as well as of reactive compatibilized polypropylene/polyamide 6 (PP/PA6) blends in a mixing zone of a co-rotating twin screw extruder on blend composition and screw rotational speed was investigated. A special process analytical set-up based on a co-rotating twin screw extruder was used, which allowed melt sampling from different positions along the operating extruder in time periods less than 10 seconds. It has been shown that the disperse particle sizes in physical blends depend crucially on the blend composition because of the increasing influence of coalescence with an increasing concentration of the disperse phase. Furthermore, the morphology of physical PP/PA6 blends depends strongly on their rheological properties. In contrast, the influence of the screw rotational speed on the morphology is minor. The resulting particle size in a mixing zone is achieved already after a short screw length. The particle size of compatibilized blends is significantly smaller than in physical blends because of the better conditions for drop break-up and the suppression of coalescence effects. Due to this, compatibilization has a stronger influence on the blend morphology than a variation of process or rheological conditions with physical blends. Furthermore, the compatibilization leads to a concurrent crystallization of the PA6 phase with the PP phase.

INTRODUCTION

Polymer melt blending is an effective and well-established method to design new materials with tailor-made properties. However, owing to the chemical nature of macromolecules, most polymers are thermodynamically immiscible. Hence, in the mixing of polymers, mostly disperse systems are formed, in which the minor constituent is dispersed in a matrix of the major constituent. The physical properties of such blends depend strongly on the size, the size distribution and the shape of the dispersed particles. Therefore, it is generally desired to manufacture blends with well-defined, stable and reproducible morphologies. Since the mixing of polymers is mainly accomplished in co-rotating twin screw extruders, a fundamental understanding of the morphology development during the flow in an extruder is required. However, owing to the "black-box"-like construction of an extruder it is difficult to investigate the morphology development during the mixing process.

Several techniques have been developed to solve this problem. Most of the appropriate methods are based on dead-stop experiments with subsequent screw pulling or split barrel opening. Since the time of melt sampling by use of these techniques is usually up to five minutes, morphology can undergo changes as a result of coalescence (1). Therefore, an original sampling method was developed that allows sampling

Corresponding author: W. J. MacKnight.

in time periods less than ten seconds without stopping the extruder. Using this procedure, the detection of the morphology development can be achieved nearly in real time (2).

Owing to the low intermolecular adhesion between the interfaces of immiscible polymers, a phase compatibilization is generally required to obtain stable morphologies (3). Compatibilization, as defined by Utracki (4), is a process of interfacial modification that improves the phase adhesion and allows control of the particle size. For the blend system polypropylene (PP)–polyamide 6 (PA6), it is known that a suitable compatibilization can be achieved by the use of maleic anhydride grafted polypropylene (PP-g-MAn) (5–8). The generation of copolymers of PP and PA6 at the polymer interface has been described as the mechanism of compatibilization (9–11).

This paper deals with the investigation of the morphology development of PP/PA6 blends in mixing zones of a co-rotating twin screw extruder. The materials used were analyzed to determine the rheological and interfacial properties. The determination of the interfacial tension between the blend components is important to describe compatibilization effects because phase compatibilization is accompanied by a significant decrease of this parameter (12, 13). The breaking thread method (12) was chosen to measure interfacial tensions.

A special setup based on a ZSK 40 was assembled for the mixing experiments. The influence of the concentration of the disperse phase and the viscosity ratio of blends on the blend morphology was investigated. The morphologies of uncompatibilized and compatibilized blends were analyzed and compared.

THEORY

Drop Deformation and Drop Break-up

Assuming that during the flow through a twin screw extruder, shear stress predominates, there are two dimensionless parameters important to characterize the drop break-up process (14):
the capillary or Weber number

$$We = \frac{\eta_m \cdot \dot{\gamma} \cdot D}{\sigma} \tag{1}$$

and the viscosity ratio

$$p = \frac{\eta_d}{\eta_m} \tag{2}$$

where η_m is the viscosity of the matrix phase, $\dot{\gamma}$ the shear rate, D the disperse particle diameter, σ the interfacial tension and η_d the viscosity of the disperse phase.

In model experiments, different break-up mechanisms of disperse droplets were observed. However, the most realistic mechanism is the break-up of elongated droplets caused by sinusoidal capillary wave instabilities (15–17). The theory of this mechanism is based on the fundamental work of Tomotika (18), who investigated the break-up of a Newtonian liquid cylinders in a Newtonian liquid quiescent matrix.

In this model, amplitudes α with a dominant wave number X_m:

$$X_m = \frac{\pi D_0}{\lambda_m} \tag{3}$$

grow exponentially with time.

$$\alpha = \alpha_0 e^{qt} \tag{4}$$

D_0 is the initial diameter of a cylinder, λ_m is the dominant wave length, α_0 the original amplitude and q the disturbance growth rate. The disturbance growth rate is given by *Eq 5* with Ω as the dimensionless distortion growth function, which is a tabulated function (18).

$$q = \frac{\sigma\, \Omega(\lambda, p)}{\eta_m D_0} \tag{5}$$

The time of the break-up of an elongated thread into a number of droplets with the same size can be estimated by (12)

$$t_b = \frac{\eta_m D_0}{2\Omega_m \sigma} \ln\left(\frac{1.39\, \sigma\, D_0^2}{4\, k\, T}\right) \tag{6}$$

with Ω_m as the corresponding dimensionless disturbance growth rate of the dominant wave number X_m and k as the Boltzmann constant. The values of Ω_m and X_m can be calculated from Tomotikas original equations (18), which are too space consuming to be reproduced here. *Figure 1* shows both Ω_m and X_m as a function of the viscosity ratio p.

Coalescence

Since the morphology development in a blend is influenced by both drop break-up processes and coalescence, it is necessary to consider coalescence as well. Several models were developed to describe the coalescence process in disperse systems (19–22). The basis of all of these models is the description of the collision frequency C of disperse particles in a matrix and of the probability of particle unification after collision, P_{unite}.

Assuming simple shear flow, the collision frequency, C, can be expressed as a function of the shear rate and the concentration of the disperse phase Φ (21, 23).

$$C = \frac{16}{\pi} \dot{\gamma}\, \Phi. \tag{7}$$

Janssen (17) compared different models for P_{unite} with his experimental data which he obtained by use of viscous model liquids. These models are based on theories of MacKay and Mason (19) and Chesters (21). Janssen applied expressions for:

- immobile interfaces

$$P_{unite} \sim \exp\left(-\frac{9}{32}\left[\frac{D}{h_{crit}}\right]^2 We^2\right) \tag{8}$$

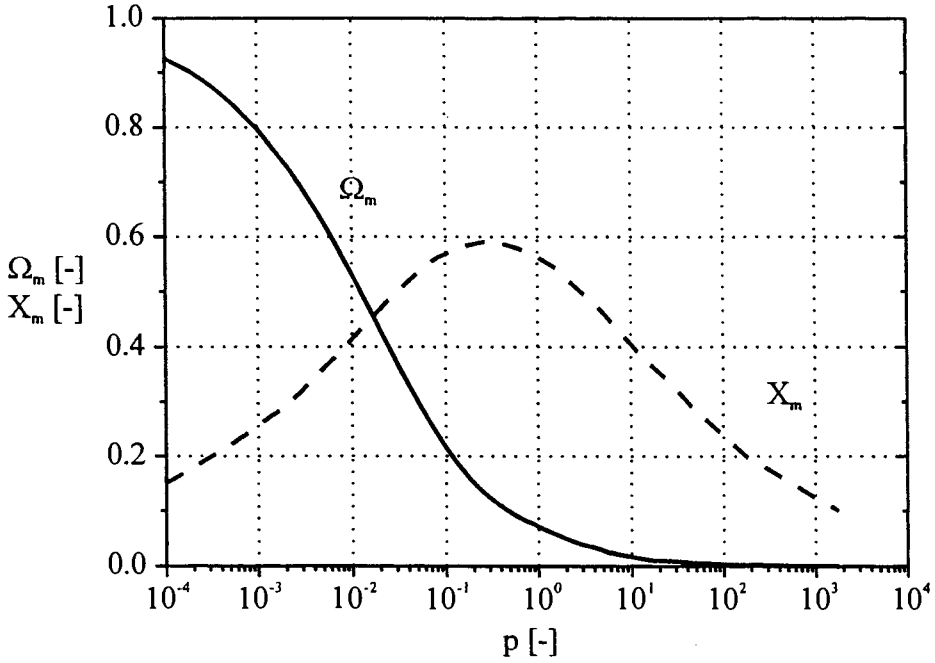

Fig. 1. Dominant wave number X_m and corresponding growth rate Ω_m of capillary instabilities versus the viscosity ratio ($p = \eta_d/\eta_m$).

- partly mobile interfaces

$$P_{unite} \sim \exp\left(-\frac{\sqrt{3}}{8}\frac{D}{h_{crit}} p\, We^{3/2}\right) \qquad (9)$$

- fully mobile interfaces

$$P_{unite} \sim \exp\left(-\frac{3}{2} We \ln\left[\frac{D}{h_{crit}}\right]\right) \qquad (10)$$

Only the partly mobile interface model corresponded within an order of magnitude with his results. Gisbergen and Meijer (24) found a qualitative correlation between their experimental results and this model as well. In contrast, Elmendorp and Van der Vegt (25) determined a good agreement between their results and the model of fully mobile interfaces. However, the model of the partly mobile interfaces was not developed at the time of their study.

All models predict that the coalescence probability will decrease with increasing Weber number and increasing particle size. Furthermore, high Weber numbers provide good conditions for drop break-up processes as well. Areas of very different shear stresses exist in an extruder causing different Weber numbers. Therefore, zones can be assumed to exist where drop break-up dominates and other zones to exist where coalescence dominates. This concept is known as two-zone mixing model (17, 26).

Experimental

Material

A blend system with PP as matrix and PA6 as disperse phase was chosen. Two different PP resins (Hostalen, Hoechst AG) and two different PA6 resins (Ultramid, BASF AG) were used.

- Polypropylene Hostalen PPT 1070 (PPT)
- Polypropylene Hostalen PPH 2150 (PPH)
- Polyamide 6 Ultramid B3 (PA6 B3)
- Polyamide 6 Ultramid B4 (PA6 B4)

To investigate the effect of compatibilization, a maleic anhydride modified polypropylene (PP-g-MAn) received from Mitsui Ltd. was used The anhydride content of this product determined by titration was 0.5 %.

- Polypropylene Admer QF 556 E (Admer)

Two physical PP/PA6 blends with different viscosity ratios were analyzed to investigate the influence of the viscosity ratio on the disperse blend morphology. Furthermore, a blend with a PP-g-MAn as matrix was analyzed to investigate the effect of compatibilization (*Table 1*).

Viscosity Measurements

The viscosity data of each component were obtained using a rotational rheometer Rheometrics RMS 800

Table 1. Polymer Blends Used in This Study.

Blend	Matrix Phase (PP)	Disperse Phase (PA6)	
PPH/PA6 B3	PPH	PA6 B3	uncompatibilized
PPT/PA6 B4	PPT	PA6 B4	uncompatibilized
Admer/PA6 B4	Admer	PA6 B4	compatibilized

operating in oscillation mode with a parallel plate configuration. The plate diameter was 25 mm. The measured values were fitted using the Carreau-Yasuda equation (27)

$$\eta = (\eta_0 - \eta_\infty)\left(1 + \left(\frac{\dot{\gamma}}{\dot{\gamma}_c}\right)^a\right)^{\frac{n-1}{a}} \qquad (11)$$

where η_0 is the zero-shear-rate viscosity, η_∞ the infinite-shear-rate viscosity, $\dot{\gamma}_c$ a constant (the crossing of the line represents zero-shear-rate viscosity and the line represents the power-law viscosity at high frequency), a is a dimensionless parameter that describes the transition region between the zero-shear-rate region and the power-law region and n is the power-law exponent.

Interfacial Tension

In recent years the breaking thread method has been applied frequently to determine interfacial tensions between melts of immiscible polymers (28, 29). Using this method Elemans *et al.* (12) found a significant decrease of the interfacial tension between polystyrene and polyethylene by adding a polystyrene-polyethylene-diblock-copolymer as compatibilizer to the system. Cho *et al.* (30) investigated the effect of end-sulfonated polystyrene on the interfacial tension in the system polyamide 6/polystyrene.

Fibers with a constant diameter of approximately 30 μm were prepared using a melt spinning apparatus. The fibers were annealed for 24 h at 100°C in a vacuum oven. Matrix sheets of PP with a dimension of 10 × 10 × 0.5 mm were made by compression molding. The thread was placed between two sheets at room temperature. Afterwards the system was placed in a Linkam hot stage. Prior to the breaking thread experiments, the systems were annealed for 10 min at a temperature close to the melting point of the thread to minimize recoiling effects during the melting of the PA6 thread. Subsequently, the system was heated to a temperature of 260°C with a heating rate of 90 K/s. The observation of growing distortions was carried out using a Zeiss optical microscope equipped with a CCD camera. Using *Eq 4*, the distortion growth rate q was determinated by the growth of the amplitude with time. The interfacial tension σ was calculated using *Eq 5*.

Extrusion

Prior to the mixing experiments, the PA6 pellets were dried under vacuum at 90°C for 12 h. Two gravimetric screw feeders were used. The average barrel temperature was 260°C for the PPH/PA6 B3 blend and 240°C for the PPT/PA6 B4 and the Admer/PA6 B4 blend. The total throughput in all experiments was 15 kg/h. Two different extruder configurations were assembled to investigate the morphology and the morphology development, respectively, in the mixing zone of a co-rotating twin-screw extruder (Werner & Pfleiderer ZSK 40).

In the first series the influence of the disperse phase concentration, the viscosity ratio and the effect of a compatibilizer on the blend morphology of three different PP/PA6 blends was investigated. In this set-up, the extruder was equipped with one sampling device. After a long zone of conveying elements to reach the equilibrium state of drop break-up and coalescence, a mixing zone of KB 45/5/20 kneading elements was assembled. The sampling was carried out at the end of this mixing zone (*Fig. 2*). The screw rotational speed in all tests was 100 rpm. The disperse phase concentrations of the PPH/PA6 B3 and PPT/PA6 B4 blend was varied in a range from 0.25 to 12 wt% PA6, the disperse phase concentrations of the Admer/PA6 B4 blend were 4, 8 and 12 wt%.

In the second series, the morphology development along a mixing zone for the different PP/PA6 blends was analyzed. To investigate the morphology development in a mixing zone, a set-up with three different sampling positions was assembled at the end of the extruder (*Fig. 3*). A throttle valve was used to achieve

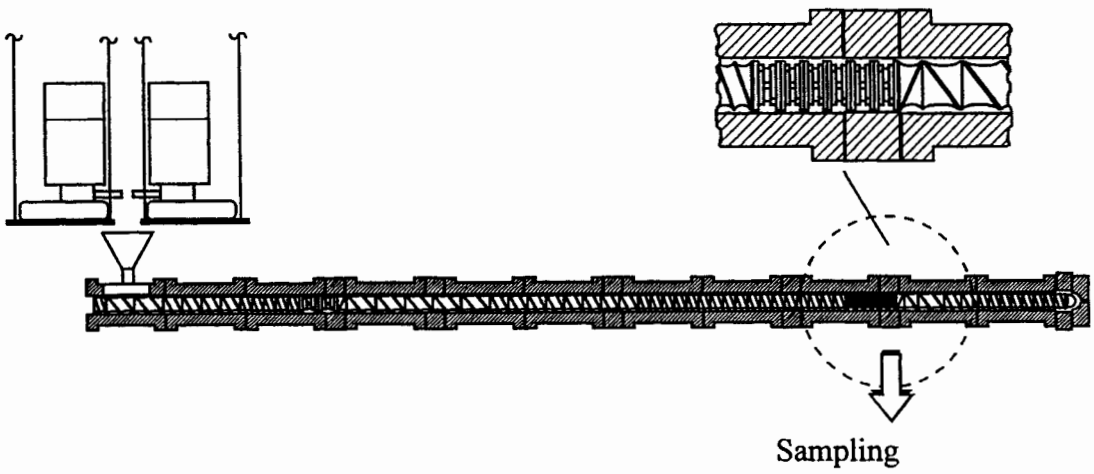

Fig. 2. Extruder barrel with screw and one sampling position.

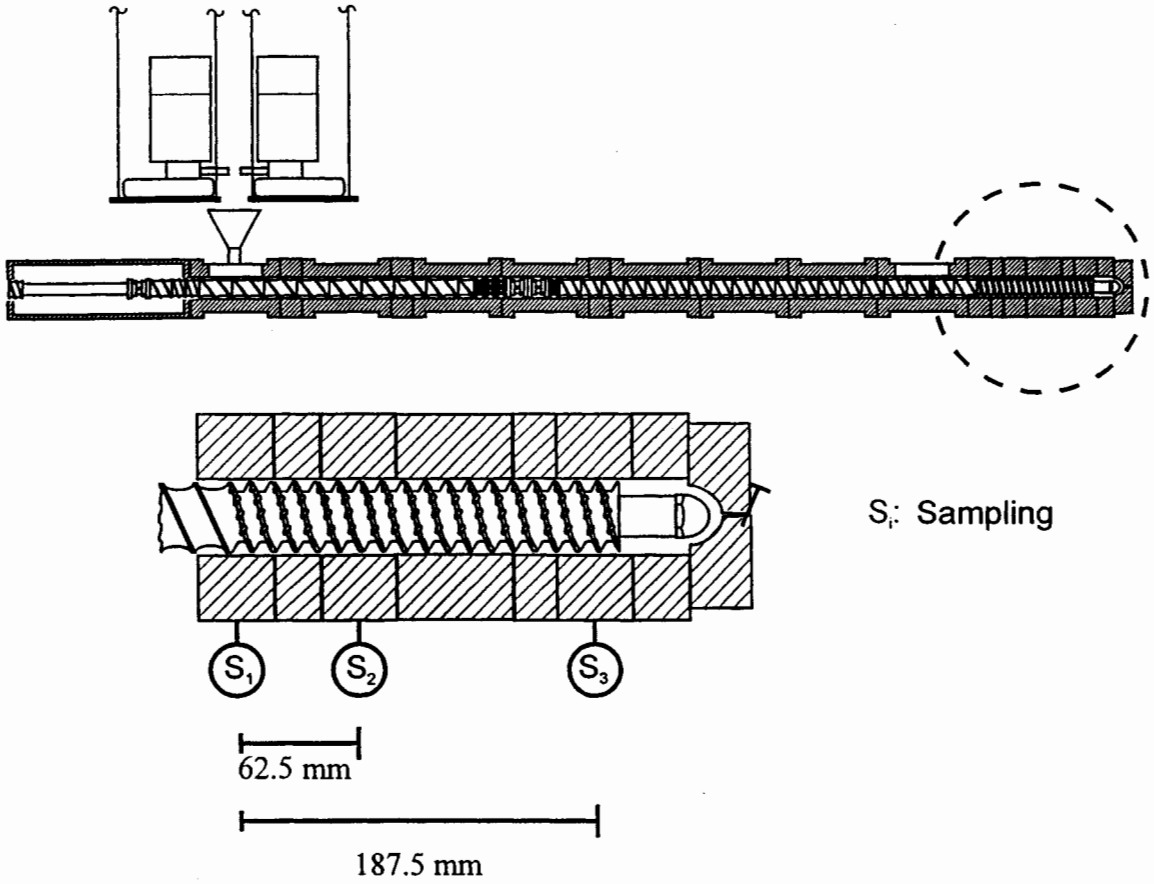

Fig. 3. Extruder barrel with screw and three sampling positions.

a filled mixing zone in all experiments. The mixing zone consisted of screw-mixing-elements (SME). The concentration of the disperse PA6 phase was in all experiments 5 wt%. For the tests with the PPT/PA6 B4 and the Admer/PA6 B4 blend, screw rotational speeds of 200, 250 and 300 rpm were used. For the tests with the PPH/PA6 B3 blend only a screw speed of 200 rpm was employed.

Morphology

Melt samples were taken from different positions along the extruder to investigate the morphology of the blends. The exact sampling procedure has been described elsewhere (2). The samples were cryo-cut at -20°C using a microtome. Micrographs of these samples were made by using a Zeiss Gemini 870 scanning electron microscope (SEM) at 10 kV of accelerating voltage. To obtain a good contrast, the disperse PA6 particles were etched with formic acid and the samples were sputtered with gold. The micrographs were analyzed by using an automatic image analyzer Leica Quantimet 570 to determine the average particle size. At least 1000 particles were counted since it has been shown that this number is necessary to obtain a sufficient accuracy (2).

RESULTS AND DISCUSSION

Rheology

Viscosity measurements were carried out at 240, 260 and 270°C. In *Figs. 4* and *5* are shown the appropriate viscosity data. The data are fitted using the Carreau-Yasuda function. The Carreau-Yasuda parameters for all materials at 260°C are listed in *Table 2*.

The viscosity ratios p were obtained by the division of the Carreau-Yasuda equations of PA6 by the Carreau-Yasuda equations of PP. In *Fig. 6* the viscosity ratios at 240, 260 and 270°C are plotted versus the temperature.

It has been reported by Wu (31) who investigated a polyamide 6,6/ethylene-propylene rubber blend that drop break-up is most probable in the range of the viscosity ratio between $p = 0.1$ and $p = 1$ and that the number average particle diameter increases with increasing viscosity ratio ($p > 1$). Taking this result into account, the rheological conditions for drop break-up of the PPH/PA6 B3 blend ($0.1 < p < 0.7$) are better than those of the PPT/PA6 B4 blend ($3.8 < p < 6.5$).

Interfacial Tension

Figure 7 depicts a uniform break-up of a PA6 B4 thread in a PPT matrix. After equal time intervals of

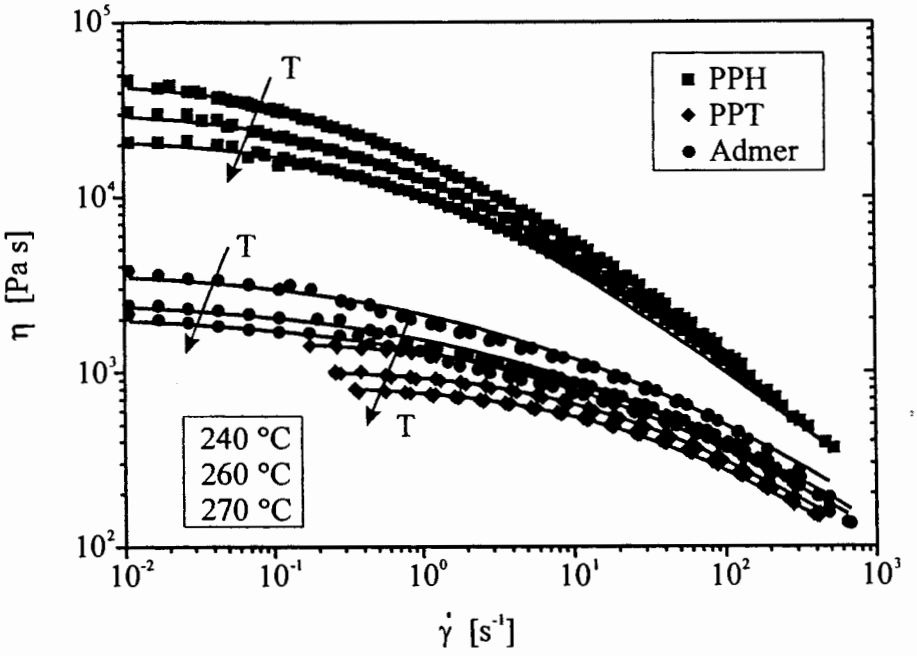

Fig. 4. Viscosity data of the polypropylenes and their Carreau-Yasuda fits.

60 s images of the growing distortions were recorded. According to *Eq 4*, the growth rate q of the distortion was calculated from the slope of the line and obtained by plotting log $(2\alpha/D_0)$ versus time. In this equation D_0 is the original thread diameter. The calculated interfacial tensions of the PPT/PA6 B4 and the PPH/PA6 B3 blend are listed in *Table 3*. Taking an accuracy of 10% (12) into account, both measured interfacial tensions can be assumed to be similar.

In contrast, *Fig. 8* depicts a PA6 B4 thread imbedded in an Admer (PP-g-MAn) matrix. The thread shows slight distortions after 5 min. However, the distortions stop growing after a certain time and even after a period of 75 min the thread does not break. A similar effect was observed by Sundararaj and Macosko (32) who investigated the system polyamide 6,6 and maleic anhydride grafted polystyrene. The experiment indicates that during the measurement immobilization of the interfaces occurs, probably due to chemical reactions of the components at the interface.

Although the observed behavior does not allow the determination of a defined value of interfacial tension

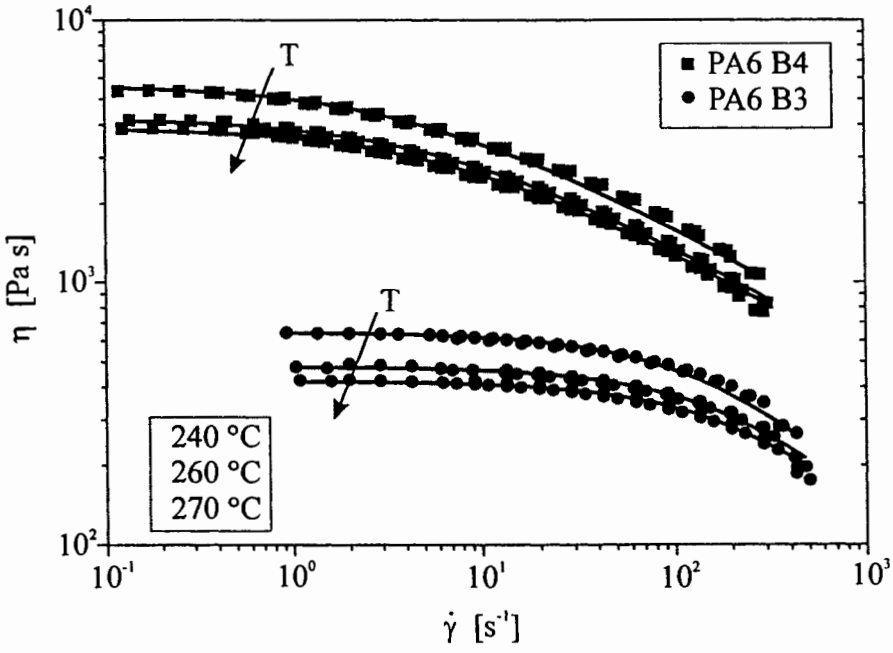

Fig. 5. Viscosity data of the polyamides and their Carreau Yasuda fits.

Table 2. Parameters From the Fitting of the Viscosity Data at 260°C With Carreau Yasuda.

	PPH	PPT	Admer	PA6 B3	PA6 B4
η_0 [Pa s]	31678.06	1065.38	2656.57	488.49	4318.37
η_x [Pa s]	0.1	0.01	0.06	0.04	9.93
$\dot{\gamma}_c$ [s^{-1}]	0.59	13.35	13.94	296.31	7.75
n [–]	0.34	0.45	0.35	0.23	0.58
a [–]	0.62	0.64	0.37	0.95	0.79

when using the breaking thread method, this result shows the strong effect of compatibilization at the interface of the blend components. Taking this result into account, it might not be exact to use degrees of interfacial tension that are obtained by the breaking thread method in the classical sense to determine effects of compatibilization when covalent chemical bondings at the interface of immiscible polymers are possible.

Effect of the Blend Composition on the Phase Morphology

Figure 9 shows that at PA6 concentrations ≤ 0.5 wt% the equivalent particle diameter (ECD) of the PPH/PA6 B3 blend is lower than the ECD of the PPT/PA6 B4 blend. However, at PA6 concentrations > 2 wt% the effect is opposite, the average ECD of the PPH/PA6 B3 blend is higher than the average ECD of the PPT/PA6 B4 blend. Referring to Wu (31), drop break-up is most probable at a viscosity ratio close to unity. Thus, in the PPH/PA6 B3 blend ($0.1 < p < 0.7$) a smaller ECD can be expected compared to the PPT/PA6 B4 blend ($3.8 < p < 6.5$), observed at low PA6 concentrations. The probable reason for the higher ECD at larger PA6 concentrations in both blend systems is coalescence effects. The influence of coalescence rises with the concentration of the disperse component due to the higher collision probability (*Eq 6*).

Nevertheless, *Eqs 8* to *10* provide no explanation why the probability of particle unification after collision P_{unite} for the PPH/PA6 B3 blend is obviously higher than for the PPT/PA6 B4 blend. However, Esseghir *et al.* (33) observed that the effect of coalescence is stronger in blends with a highly viscous matrix phase. The authors explained that this effect is due to higher laminar flow stresses in a highly viscosity matrix which forces the dispersed domains to meet and to coalesce.

Furthermore, *Fig. 9* shows that the particle size of the Admer/PA6 B4 blend is significantly smaller compared to the two uncompatibilized blend systems. This finding indicates that under the investigated mixing conditions, the compatibilization causes better conditions for drop break-up processes. This effect is in accordance with the results of Sundararaj and Macosko (32) who observed smaller particle sizes

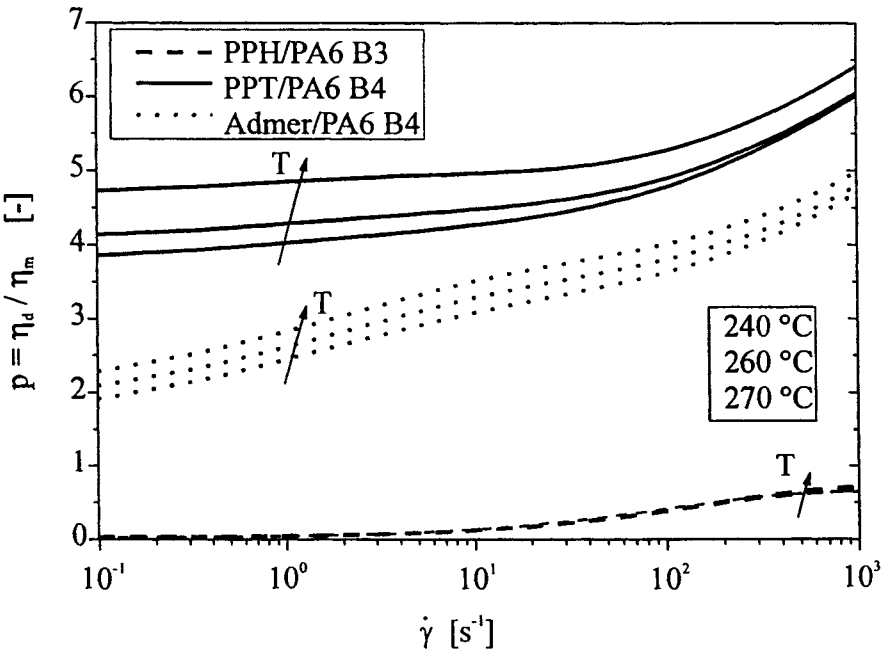

Fig. 6. Viscosity ratios ($p = \eta_d/\eta_m$) of the blends.

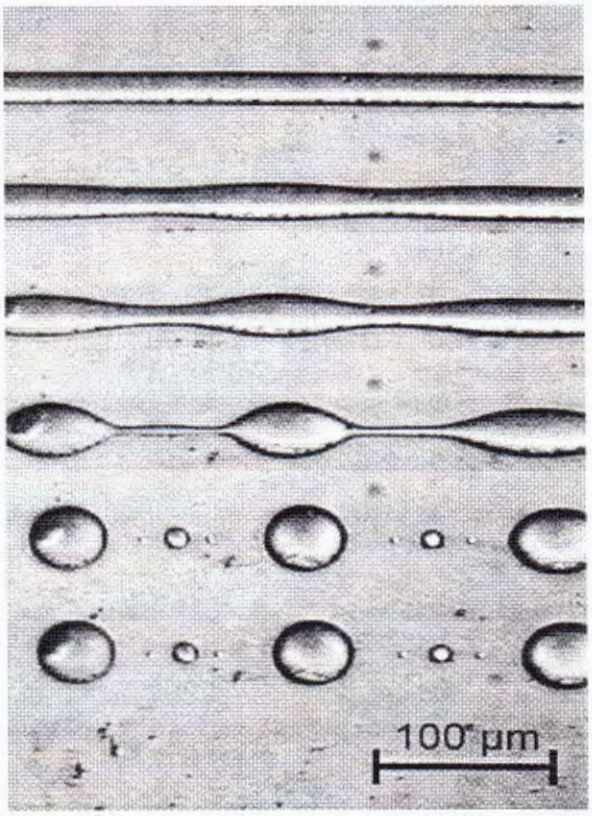

Fig. 7. Disintegration of a PA6 B4 thread in a PPT matrix at 260°C.

at the low concentration limit of a nonreactive polyamide/polystyrene blend in reactive polyamide 6,6/polystyrene-maleic anhydride blends.

Further agreement with the results of Sundararaj and Macosko (32) is the lack of dependence of the particle size on the PA6 concentration in Admer/PA6 B4 blends. The authors found that by reactive compatibilization coalescence is suppressed up to concentrations of the disperse phase of 20 wt% and that the particle size at this concentration is not dependent on the disperse phase concentration.

The micrographs in *Figs. 10a* to *10c* show the morphology of samples of the three investigated blend systems with the composition 88 wt% PP and 12 wt% PA6. The effect of the compatibilization on the size of the disperse particles is obvious. Furthermore, *Fig. 10* shows a significant difference in the particle shape between the PPT/PA6 B4 and the PPH/PA6 B3 blend. The disperse domains in the PPH/PA6 B3 blend are much more elongated than in the PPT/PA6 B4 blend expressed by the aspect ratio AR.

$$AR = \frac{particle\ length}{particle\ breadth} \tag{12}$$

The development of the mean AR's and their standard deviations for the physical blends (*Fig. 11*) demonstrates that at PA6 concentrations > 4 wt% disperse domains in PPH/PA6 B3 blends are elongated whereas domains in PPT/PA6 B4 blends remain almost spherical. Taking the theory of the Weber number (*Eq 2*) into account, the blend with the viscosity ratio close to unity (PPH/PA6 B3: $0.1 < p < 0.7$) has better conditions for drop break-up than the blend system with the higher viscosity ratio (PPT/PA6 B4: $3.8 < p < 6.5$). However, the results of Esseghir *et al.* (33) show that coalescence effects rise with an increase of the matrix phase viscosity. These two contradictory effects may be the reason that the particles in the PPH/PA6 B3 blend are much more elongated but not smaller than in the PPT/PA6 B4 blend.

Morphology Development Along a Mixing Zone in an Extruder

Figure 12 shows the evolution of the number average ECD along the investigated mixing section. The development of the ECD of the PPT/PA6 B4 blend shows that at all screw speeds the significant dispersion of the particles takes place in the 62.5 mm between the first and the second sampling position. The reduction of the mean ECD between the second and the third sampling position is not significant. Furthermore, *Fig. 12* depicts the interesting effect that in the PPT/PA6 B4 blend the average ECD at the first sampling position at 250 rpm is significantly higher than at 200 rpm. At 300 rpm, the melt contained even solid particles at this position (*Fig. 13*) and made a quantitative analysis of these samples impossible. The increase of the particle diameter with an increase of the screw rotational speed is unusual, since an increase in the screw speed causes in general a higher energy input (34, 35), which should cause a better melting behavior. The reason for the worsening of the plastification by an increasing screw rotational speed is probably a decreasing backup length in the melting zone with increasing screw speed. Because of this effect, the residence time in the melting zone, and therefore the melting efficiency, decrease with an increasing screw rotational speed. At the second sampling position only minor differences in the particle

Table 3. Interfacial Tension Data Determined at 260°C Via the Breaking Thread Method.

Matrix phase (PP)	Thread phase (PA6)	p [–]	X_{exp} [–]	X_m [–]	Ω_m [–]	σ [mN/m]
PPH	PA6 B3	0.015	0.44	0.45	0.4741	10.7
PPT	PA6 B4	4.053	0.50	0.48	0.0351	9.2
Admer	PA6 B4	1.626	—	0.54	0.0567	no break

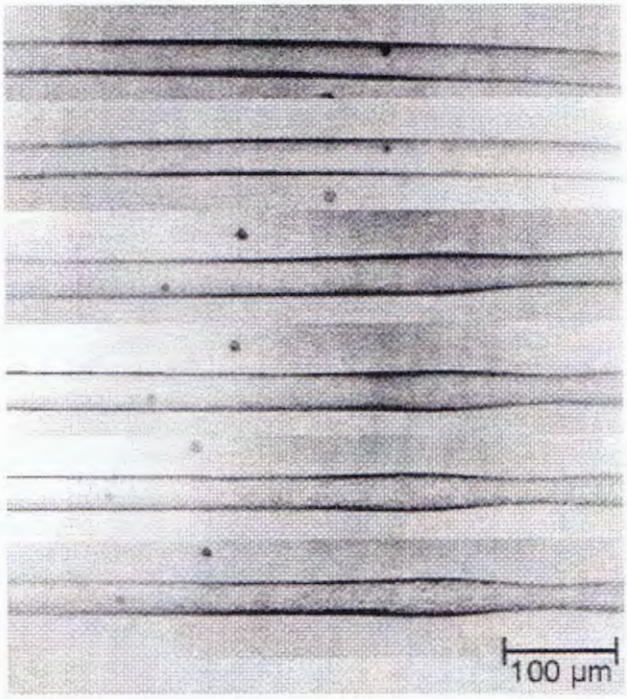

Fig. 8. PA6 B4 thread in an Admer matrix at 260°C.

size between the different screw rotational speeds and at the third sampling position exist. No more differences in the particle size are present.

The average ECD of the PPH/PA6 B3 blend at all sampling positions is smaller than the average ECD of the PPT/PA6 B4 blend at 200 rpm. This is a further indication that the rheological properties for drop break-up of the blend with a viscosity ratio close to unity (PPH/PA6 B3) are better than those of a blend with a viscosity ratio larger than one (PPT/PA6 B4). Like the tests with the PPT/PA6 B4 blend, the main changes in the morphology occur in the first 62.5 mm of the mixing zone.

The ECD's of the Admer/PA6 B4 Blend are at all sampling positions significantly smaller than those of the uncompatibilized blends. However, the experiments with the Admer/PA6 B4 blend show that there is no effect of the screw rotational speed on the morphology. Furthermore, there is no significant change of the morphology along the mixing zone. The fact that the screw configuration used contained only a melting zone and a long section of conveying elements prior to the mixing section which have almost no mixing efficiency indicates that in the compatibilized Admer/PA6 B4 blend the morphology formation occurs mainly already in the melting zone. This finding is in accordance with the results of Sakai (36), who found by the use of a PP-g-MA/PA blend that the main dispersion occurs in the melting zone.

Effect of Phase Compatibilization on the Crystallization Behavior (DSC)

Thermal analysis was carried out using a DSC 7 (Perkin-Elmer) in nitrogen atmosphere to study the influence of the melting and the crystallization behavior of the blends. Two heating and one cooling cycle were done in the temperature range from –60 to 250°C at a rate of 10 K/min.

Figure 14 shows the cooling curves of PPT, PA6 B4 and the PPT/PA6 B4 blends whereas *Fig. 15* shows the cooling curves of Admer, PA6 B4 and the Admer/PA6 B4 blends. In *Fig. 14* it can be seen that the crystallization temperature of the PPT matrix is slightly

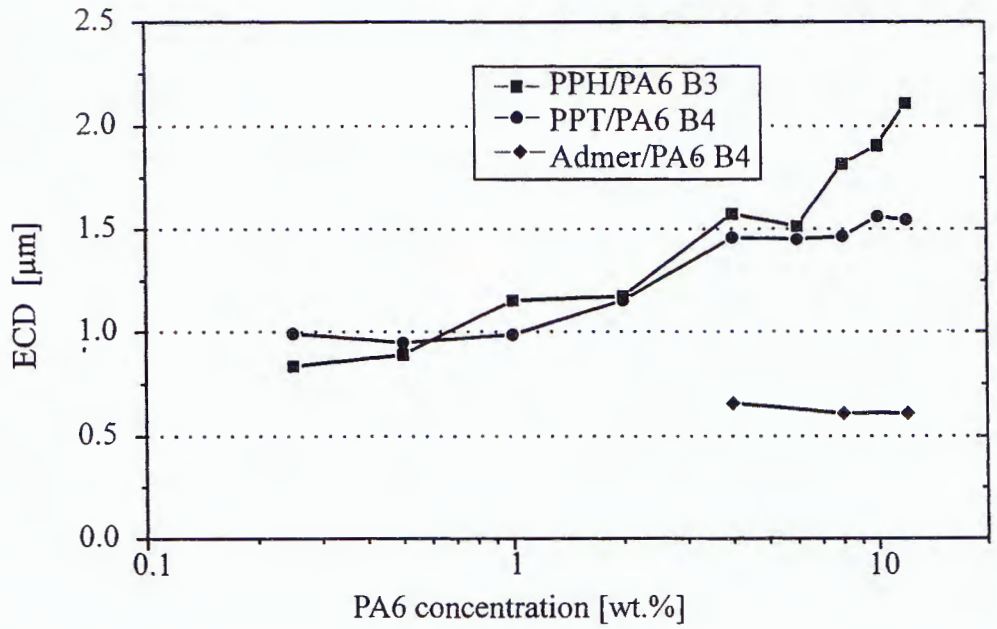

Fig. 9. Average Equivalent Circle Diameter (ECD) of the investigated PP/PA6 blends versus the PA6 concentration.

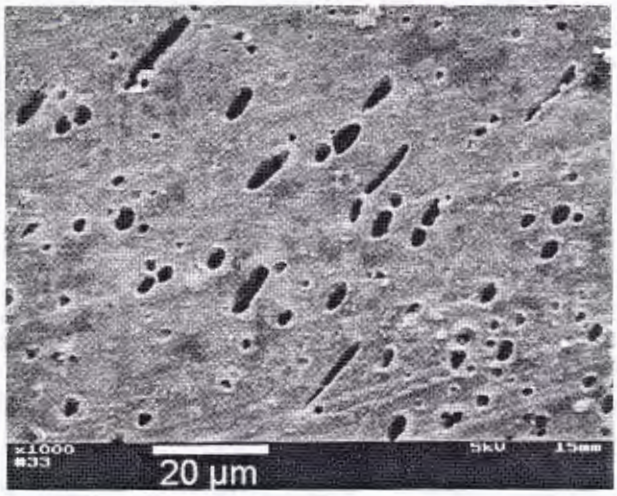

(a)

Fig. 10a. Micrograph of a sample of a PPH/PA6 B3 blend with a composition of 88 wt% PP and 12 wt% PA6.

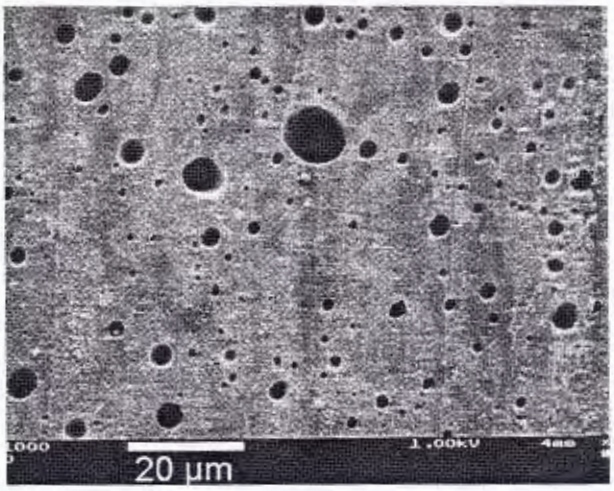

(b)

Fig. 10b. Micrograph of a sample of a PPT/PA6 B4 blend with a composition of 88 wt% PP and 12 wt% PA6.

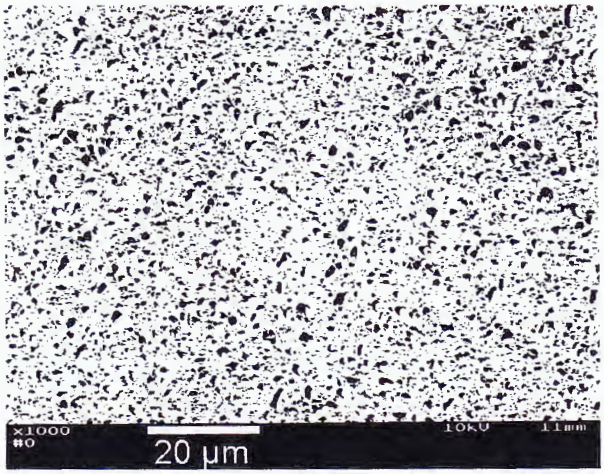

(c)

Fig. 10c. Micrograph of a sample of an Admer/PA6 B4 blend with a composition of 88 wt% PP and 12 wt% PA6.

increasing with an increasing content of the PA6 phase due to the nucleating activity of the dispersed PA6 particles. This finding is in accordance with the results of Vanneste *et al.* (37). *Figure 15* shows that in the Admer/PA6 B4 blend no crystallization peak arises at the typical crystallization temperature of the PA6 phase. However, the second melting scan of the Admer/PA6 B4 blends (*Fig. 16*) shows a clear melting peak at the typical PA6 temperature of 221.1°C. This unusual behavior is in accordance with results of other authors (37–39). Moon *et al.* (38) explained this effect by concurrent crystallization of the PA6 with the PP-g-MAn phase. The reason for this kind of crystallization is probably the reduction of the PA6 particle size. A smaller disperse particle size decreases the probability of the existence of units of a certain heterogeneity and, as a result, the possibility of crystallization at the usual crystallization temperature.

CONCLUSIONS

Because of the complexity of the flow and mixing behavior in an extruder the development of suitable models about the morphology development during the mixing in an extruder is a very complicated matter. Furthermore, the black-box-like construction of twin-screw extruders makes it very difficult to obtain experimental data to verify theoretical models. The determination of information about the dynamics of morphology development of disperse blend systems in an extruder was the main emphasis of this study. PP/PA6 was used as the disperse blend system.

Since the PPH/PA6 B3 blend has the finer morphology at low PA6 concentrations compared to the PPT/PA6 B4 blend and a coarser morphology at high PA6 concentrations, it has been shown that Wu's statement that blends with a viscosity ratio close to unity have a finer disperse morphology than blends with a high viscosity ratio is not in general valid. The effect of the blend composition and the effect of coalescence at higher concentrations, respectively is also very important.

The investigation of the morphology development along a mixing zone showed that the influence of the screw rotational speed on the blend morphology is minor. In contrast, the influence of the rheological parameters of the blend components is important. It has further been shown that the main changes in particle size occur in the first 62.5 millimeters of the mixing zones, whereas there is no significant reduction of the disperse particle size after the second sampling position.

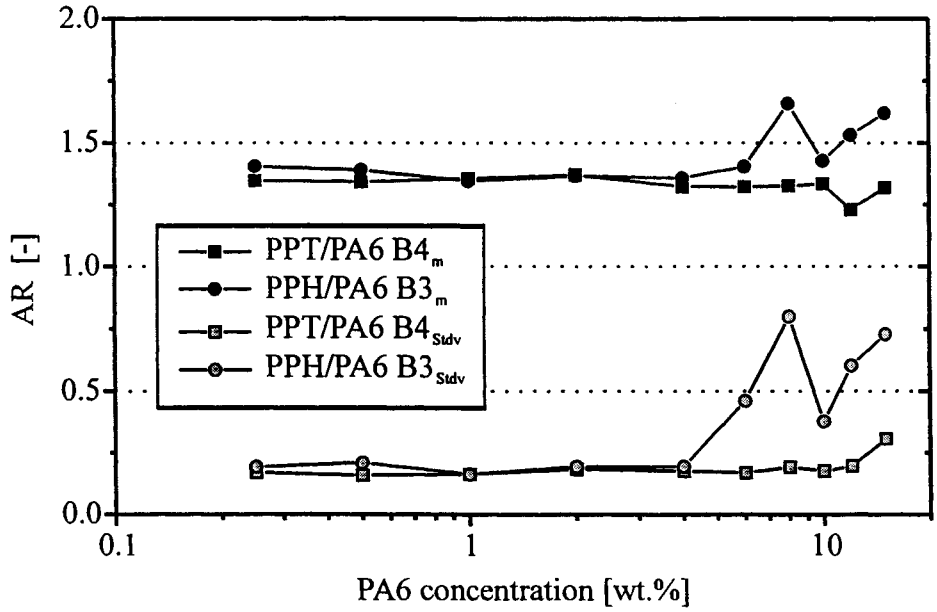

Fig. 11. Average Aspect Ratios (AR) and their standard deviations of the PP/PA6 blends versus the PA6 concentration.

The compatibilization of a PP/PA6 blend by the use of maleic anhydride grafted polypropylene (Admer) supports the drop break-up process and suppresses the coalescence process in the investigated range of composition. The consequence is a drastic reduction of the particle size compared to the uncompatibilized blends. Processing conditions or the blend composition have no significant effect on the blend morphology in compatibilized blends. A further effect of the compatibilization is the concurrent crystallization of the PA6 with the PP-g-MAn as a result of the drastic reduction of the disperse particle size.

For general conclusions more experimental work with different blend systems is necessary.

ACKNOWLEDGMENTS

This work was financially supported by the German Federal ministry for Education, Science, Research and Technology (BMBF-project 03M4080 6). Additionally the authors are grateful to the Werner & Pfleiderer GmbH, Stuttgart, for discussion on parts of this topic and material support. Thanks also to the Hoechst AG, Frankfurt, and BASF AG, Ludwigshafen

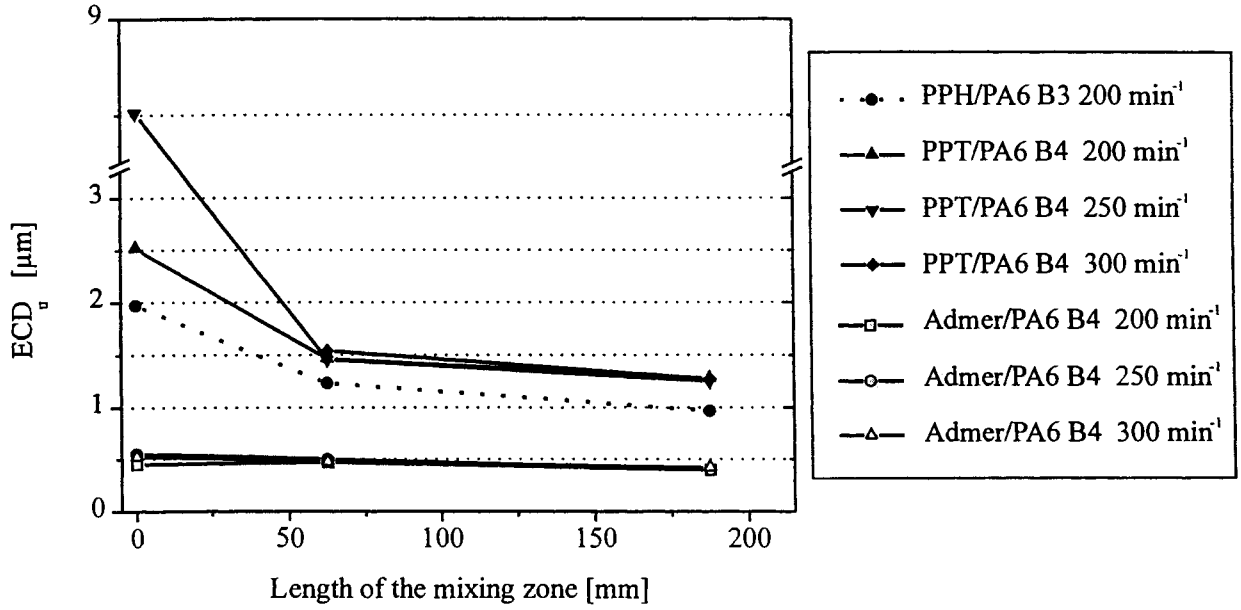

Fig. 12. Development of the average Equivalent Circle Diameter (ECD) of the PP/PA6 blends along the mixing zone.

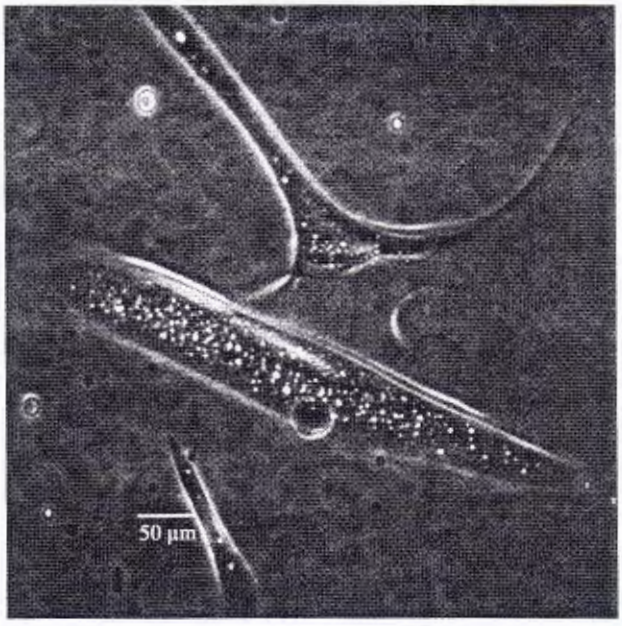

Fig. 13. Solid PA6 B4 particles in a PPT matrix at a screw rotational speed of 300 rpm at the first sampling position.

for material support. Furthermore, we thank Mrs. Liane Häussler for DSC measurements.

NOMENCLATURE

Admer = Admer QF 556 E.
PA6 = Polyamide 6.
PA6 B3 = Ultramid B3.
PA6 B4 = Ultramid B3.
PP = Polypropylene.
PP-g-MAn = Maleic anhydride grafted polypropylene.
PPH = Hostalen PPH 2150.
PPT = Hostalen PPT 1070.
a = Dimensionless parameter.
AR = Aspect ratio.
C = Collision frequency.
D = Drop diameter.
D_0 = Initial thread diameter.
ECD = Equivalent circle diameter.
k = Boltzmann constant.
n = Power law exponent.
p = Viscosity ratio.
P_{unite} = Probability of unification of particles after a collision.
q = Disturbance growth rate.
T = Temperature.
t_b = Time for thread break-up.
We = Weber number.
X_m = Dominant wave number.
α, α_0 = Amplitude, original amplitude.
$\dot{\gamma}$, $\dot{\gamma}_c$ = Shear rate, constant shear rate.
η, η_0, η_∞ = Viscosity, zero-shear-rate viscosity, infinite-shear-rate viscosity.
η_d, η_m = Disperse and matrix phase viscosity.
λ_m = Dominant wave length.
σ = Interfacial tension.
Ω; Ω_m = Dimensionless disturbance growth rate.

REFERENCES

1. A. De Loor, P. Cassagnau, A. Michel, and B. Vergnes, *Intern. Polym. Proc.* **IX 3**, 211 (1994).
2. O. Franzheim, M. Stephan, T. Rische, P. Heidemeyer, U. Burkhardt, and A. Kiani, *Adv. Polym. Tech.*, **16(1)**, 1 (1997).

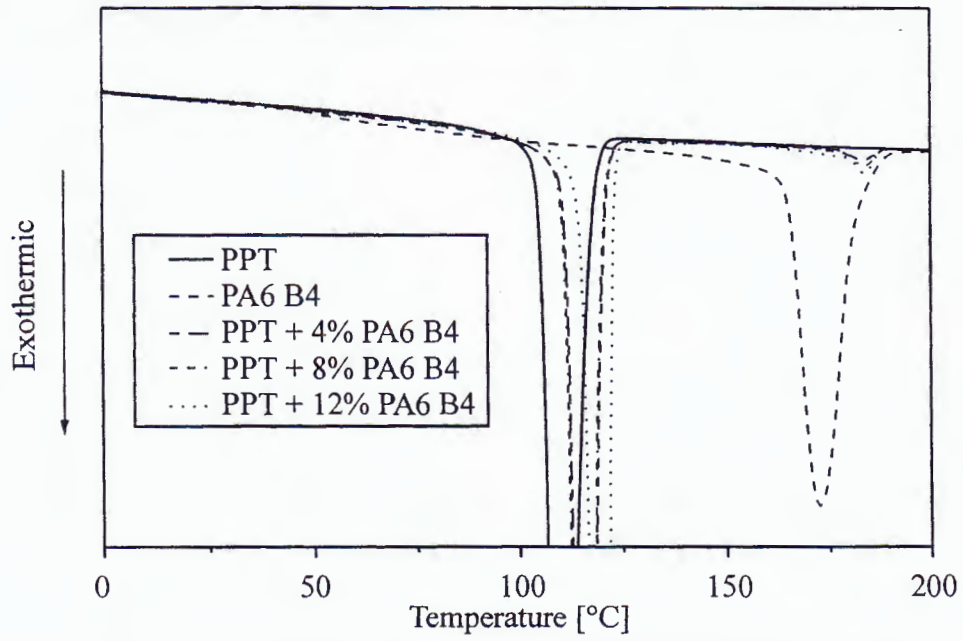

Fig. 14. DSC cooling thermograms of PPT/PA6 B4 blends with various PA6 concentrations (cooling rate 10 K/min).

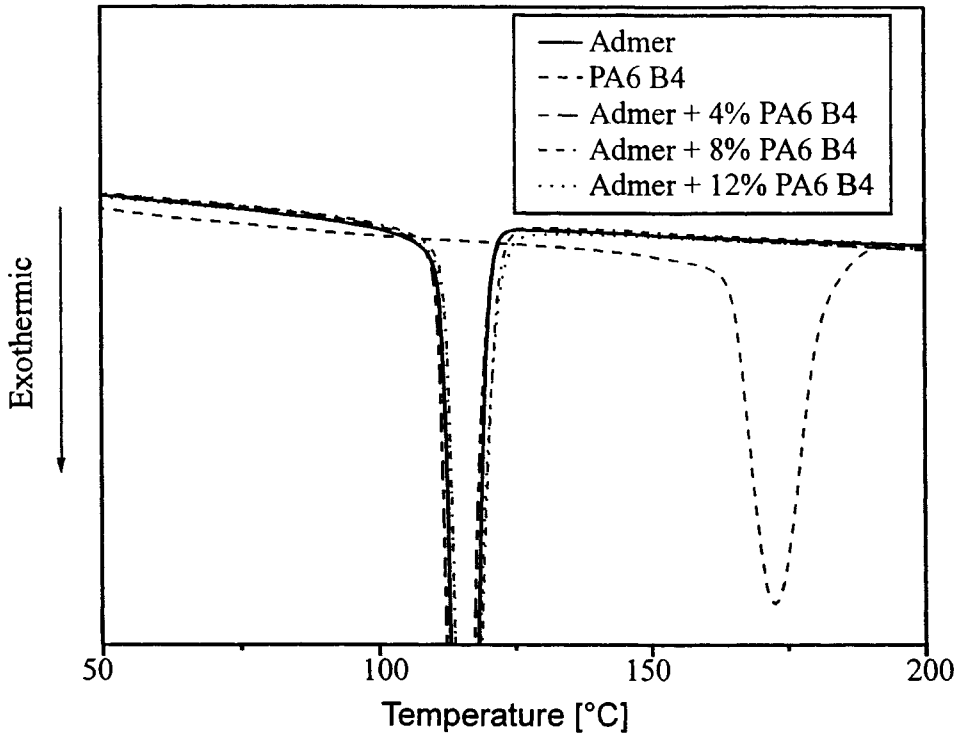

Fig. 15. DSC cooling thermograms of Admer/PA6 B4 blends with various PA6 concentrations (cooling rate 10 K/min).

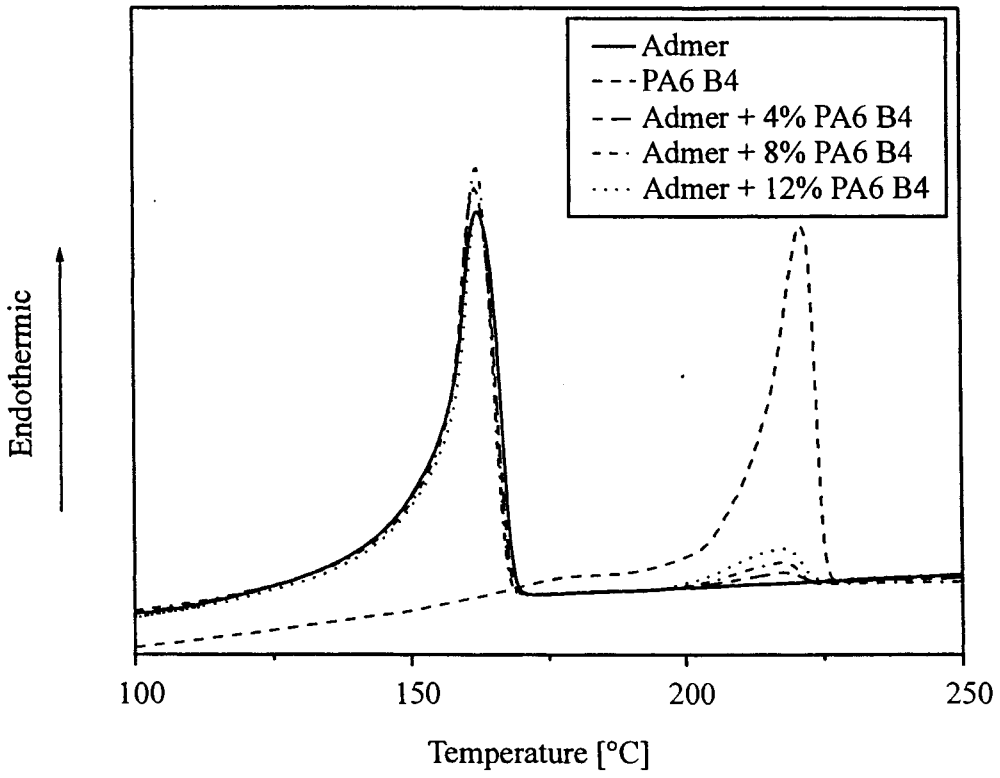

Fig. 16. DSC second heating thermograms of Admer/PA6 B4 blends with various PA6 concentrations (heating rate 10 K/min).

3. R. Legras, P. Marechal, and J. M. Dekoninck, *SPE ANTEC Tech. Papers*, 1504 (1994).
4. L. A. Utracki, *Polymer Alloys and Blends: Thermoynamics and Rheology*, Carl Hanser Publishers, Munich, Vienna, New York (1989).
5. F. Ide and A. Hasegawa, *J. Appl. Polym. Sci.*, **18**, 963 (1974).
6. T. Nishio, Y. Suzuki, K. Kojima, and M. Kakugo, *J. Polym. Eng.*, **10 (1-3)**, 123 (1991).
7. M. Xanthos, *Reactive Extrusion*, Hanser Publishers, Munich, Vienna, New York, Barcelona (1992).
8. A. Gonzalez-Montiel, H. Keskkula, and D. R. Paul, *J. Polym. Sci., Polym. Phys.*, **33 (12)**, 1751 (1995).
9. R. Mühlhaupt and J. Rösch, *Kunststoffe*, **84**, 1153 (1994).
10. M. van Duin, *9th Annual PPS Meeting*, Manchester (1993).
11. H. G. Fritz, Q. Cai, and U. Bölz, *Kautschuk Gummi Kunststoffe*, **49 (2)**, 88 (1996).
12. P. H. M. Elemans, J. M. H. Janssen, and H. E. H. Meijer, *J. Rheol.*, **34**, 1311 (1990).
13. J. Kirjava, T. Rundquist, R. Holst-Miettinen, M. Heino, and T. Vainio, *J. Appl. Polym. Sci.*, **55**, 1069 (1995).
14. H. P. Grace, 3rd Eng. Found. Conf. Mixing, Andover, N.H. (1971), republished in: *Chem. Eng. Commun.*, **14**, 225 (1982).
15. J. M. Ottino, *Phys. Fluids A*, **3 (5)**, 1417 (1991).
16. M. Tjahjadi and J. M. Ottino, *J. Fluid Mech.*, **232**, 191 (1991).
17. J. M. H. Janssen, PhD thesis TU Eindhoven, The Netherlands (1993).
18. S. Tomotika, *Proc. Roy. Soc.*, **A 150**, 322 (1935).
19. G. D. M. MacKay and S. G. Mason, *Canad. J. Chem. Eng.*, **41**, 203 (1963).
20. J. J. Elmendorp, PhD thesis, TH Delft, The Netherlands (1986).
21. A. K. Chesters, *Trans I Chem E*, **69 (A)**, 259 (1991).
22. I. Forteln and Z. Antonín, *Polym. Eng. Sci.*, **35**, 1872 (1995).
23. M. Smoluchowski, *Z. Phys. Chem.*, **92**, 129 (1917).
24. J. G. M. van Gisbergen and H. E. H. Meijer, *J. Rheol.*, **35 (1)**, 63 (1991).
25. J. J. Elmendorp and A. K. van der Vegt, *Polym. Eng. Sci.*, **26**, 1332 (1986).
26. J. M. H. Janssen and H. E. H. Meijer, *Polym. Eng. Sci.*, **35**, 1766 (1995).
27. R. B. Bird, R. C. Armstrong, and O. Hassager, *Dynamics of Polymeric Liquids Vol. 1 Fluid Mechanics*, New York, John Wiley & Sons (1987).
28. U. Sundararaj, C. W. Macosko, A. Nakayama, and T. Inoue, *Polym. Eng. Sci.*, **35 (1)**, 100 (1995).
29. A. Luciani, M. F. Champagne, and L. A. Utracki, *Polym. Netw. & Blends*, **6 (2)**, 51 (1996).
30. K. Cho, H. K. Jeon, C. E. Park, J. Kim, and U. Kim, *Polymer*, **37**, 1117 (1996).
31. S. Wu, *Polym. Eng. Sci.*, **27**, 335 (1987).
32. U. Sundararaj and C. W. Macosko, *Macromolecules*, **28**, 2647 (1995).
33. M. Esseghir, D.-W. Yu, and C. G. Gogos, *SPE ANTEC Tech. Papers, 1994* (1995).
34. *P. Heidemeyer, PhD thesis RWTH Aachen, Germany (1990).*
35. S. Tenge and D. Mewes, *13th Annual Meeting of the Polymer Processing Society (PPS)*, 1-E, Secaucus, N. J. (1997).
36. T. Sakai, *Adv. Polym. Tech.*, **14 (4)**, 277 (1995).
37. M. Vanneste, L. Ruys, and G. Groeninckx, *5th European Symposium on Polymer Blends*, 309, Maastricht, The Netherlands (1996).
38. H.-S. Moon, B.-K. Ryoo, and J.-K. Park, *J. Polym. Sci.: Part B: Polym. Phys.*, **32**, 1427 (1994).
39. T. Tang and B. T. Huang, *J. App. Polym. Sci.*, **53 (3)**, 355 (1994).